Pergamon

Polyhedron Vol. 14, No. 8, pp. 1083–1089, 1995

0277-5387/95 $9.50+0.00

0277-5387(94)00334-3

A KINETIC STUDY OF THE REACTION OF A QUASI-AROMATIC PLATINUM(II) COMPLEX WITH AROMATIC ALDEHYDES

YUAN-MING ZHANG, HUA-KUANG LIN and YUN-TI CHEN

Department of Chemistry, Nankai University, Tianjin, P.R. China

and

R. KENT MURMANN*

Department of Chemistry, University of Missouri, Columbia, MO 65211, U.S.A.

(*Received* 8 *June* 1994; *accepted* 22 *August* 1994)

Abstract—A kinetic study of the reaction of PtoylH (AH), having a quasi-aromatic $Pt_1C_3N_2$ ring, at the carbon *para* to the metal, C(12), with *para*-substituted benzaldehydes (ald) show it to be a two-step reaction producing sequentially $ACH(OH)C_6H_4R$ and $A_2CHC_6H_4R$. In dilute HCl, 1:4 v/v ethanol–water media, the first step follows the rate expression, $rate_1 = (k_{1o}+k_{1h}[H^+])[AH][ald]$ and for step 2, $rate_2 = k_2[AH][ACH(OH)C_6H_4R]$. The second step also has a positive hydrogen ion dependence, but lower precision in k_2 prevented a quantitative evaluation. In the concentration ranges used, $rate_2$ was about $500 \times rate_1$. Both rate constants tend to decrease with increasing ethanol content of the solvent. There is a clear linear free energy relationship between k_{1h} and the Hammett parameters for the substituted benzaldehydes. The activation parameters for k_1 showed a $\Delta H^\ddagger$ of around 25 kJ mol^{-1} and $\Delta S^\ddagger$ of about -170 J K^{-1} mol^{-1}. Trends in these parameters are compared with the nickel analogue.

It has been found that the complex (1,1,2,8,9,9-hexamethyl-4,6-dioxa-5-hydra-3,7,10,14-tetra-aza-cyclotetradeca-2,7,10,12-tetraene)nickel(II) (NioylH),† which contains the $[Ni_1C_3N_2]$-quasi-aromatic ring, has many interesting properties, many of which are related to the reactivity of that ring in the C(12) position[1–3] (Fig. 1). In our previous work[3] on the kinetics and the mechanism of the reaction of Nioyl with formaldehyde, it was shown to follow a three-step electrophilic substitution process. A study on the rates of reaction between Nioyl and aromatic aldehydes has recently been reported[4] which parallels this study. In this work, we describe experiments on the reaction of PtoylH with substituted aromatic aldehydes. The purpose was to understand the effect of changing metal ion and of substituents located on the benzaldehyde ring on

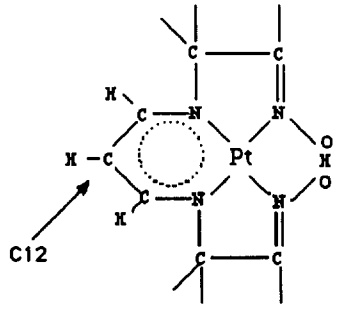

Fig. 1. Reactant molecule, PtoylH.

* Author to whom correspondence should be addressed.

† NioylH and PtoylH are abbreviations for (1,1,2,8,9,9-hexamethyl-4,6-dioxa-5-hydra-3,7,10,14-tetra-aza-cyclotetradeca-2,7,10,12-tetraene)nickel(II) and (1,1,2,8,9,9-hexamethyl-4,6-dioxa-5-hydra-3,7,10,14-tetra-aza-cyclotetradeca-2,7,10,12-tetraene)platinum(II).

the kinetics of the reaction. Toward this end, a comparison was made between the kinetic activation values and the Hammett parameters for a series of substituted benzaldehydes.

EXPERIMENTAL

Materials

PtoylH was prepared by the general method of Vassian and Murmann[5] using $NaIO_3$ in 2 M KOH solution in the oxidation to the aromatic ring. Final purification was by recrystallization from acetonitrile–water solution. The aldehydes were of A.R. quality and were additionally purified by distillation under vacuum when the substance was a liquid or by recrystallization for solids. The preparation and properties of the product were essentially the same as those given for the nickel analogue reported previously.[6] All aldehydes were continuously protected from air oxidation by maintaining a nitrogen atmosphere during storage. This was important because the reaction rates are general acid catalysed and were increased by the presence of the carboxylic acid oxidation product.

Instruments

The UV–vis spectra were recorded on a Shimadzu UV–vis spectrometer using matched quartz cells. It was not necessary to remove air from the reactant cells, providing the reaction was carried out immediately after dilution, because air oxidation of the aldehyde was relatively slow. The temperature was controlled by a thermostatted ($\pm 0.1°C$) cell. The IR spectra were recorded on a Oye Unican SP3-300 IR spectrometer. Computations for the kinetic evaluations were carried out on an AST 286 microcomputer utilizing the least-squares programs described. The agreement between replicate runs was generally $\pm 2\%$.

Selection of experimental conditions

Acidic conditions were used because the reactions of [Pt(PnAO)-6H]$^\circ$ with most of the aromatic aldehydes tried were too slow to be measured conveniently in the absence of acid. The starting complex and the products are only moderately soluble in water, thus it was necessary to use a mixed 1 : 4 (v/v) ethanol–water solvent media, which was employed throughout this study. (Note that in the Nioyl study, methanol–water solutions were used.) Traces of the corresponding carboxylic acid, formed by concurrent air oxidation, were expected to influence irreproducibly the rates of reaction, especially if high temperatures were employed. In a low acidity range, pH 3–4, the reaction was complicated by the competing self-decomposition of AH. It is known that Nioyl and Ptoyl protonate very rapidly at the hydrogen bond oxygen at higher acidities, giving AH_2^+ and that over a long period of time a complicated reaction series occurs in which the major product is A :: CH :: CH :: CH :: A^2, a conjugated dimer having an extremely intense absorption band at 508 nm (Nioyl). This dimer has been isolated, an X-ray structure reported and the mechanism of its formation studied. This undesirable reaction was found to go almost to completion when reaction was carried out in the presence of excess aldehyde in the pH range 3–4. In the acidity region used in this study, it was shown that this reaction does not take place to any appreciable extent. An additional side reaction occurs to a limited extent at long reaction times with the final product, in which it is slowly air oxidized in two one-electron steps to known compounds (unpublished results). It was found, however, that at higher acidities, 0.01–0.12 M H^+, the reaction with the aldehydes became dominant, with little decomposition of either type occurring during the 10–30 min necessary for completion and that the intense absorption band at about 508 nm caused by decomposition was apparent only after 3–4 h. Thus, the majority of the studies presented here were conducted in 0.01–0.12 M acid at 30–50°C, where the predominant reactant complex species is AH and very little disruption of the aromatic ring occurs during condensation on C(12).

REACTION ROUTE AND RATE COMPUTATION

Identification of reaction scheme

In dilute acid media (0.01–0.12 M HCl), the spectrum of AH is consistent with it being predominantly in the AH form and the changes which occur with time in the presence of aromatic aldehydes agree with that expected for a single product, $A_2CHC_6H_4R$, as shown in Fig. 2. The absorption increases continuously with time in the entire 340–440 nm region. The final product formed in solution was shown to be $A_2CHC_6H_4R$ by isolating the complex and comparing its spectrum with an authentic solid sample, establishing the essentially complete conversion of AH and RC_6H_4CHO to $A_2CHC_6H_4R$ in the acid media employed. An example of the visible spectrum of the final product in neutral alcohol solution is given in Fig. 3. Similar spectral changes were observed for all of the aldehydes used. Even in an excess of the aldehyde, the

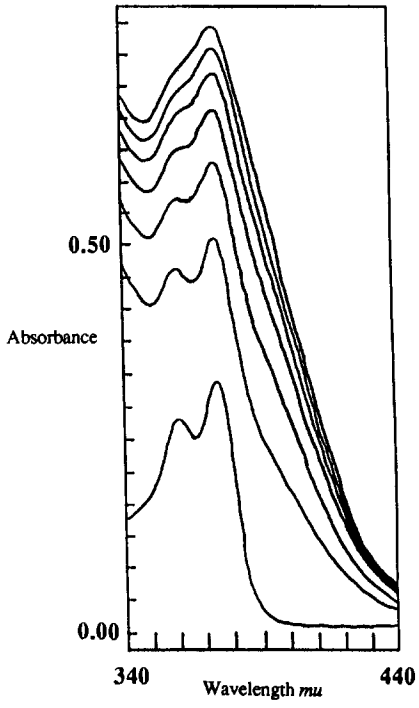

Fig. 2. Reaction of AH with benzaldehyde: absorption increases with time (3-min intervals, 28.2°C).

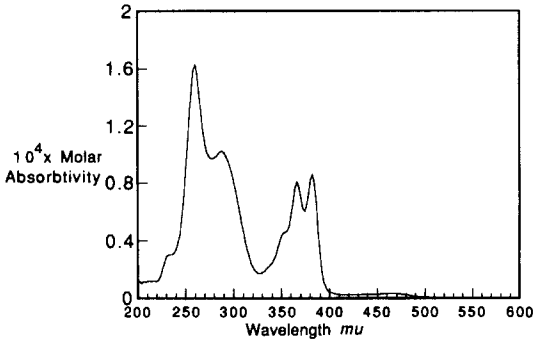

Fig. 3. Visible spectrum of $A_2CHC_6H_4$—H in neutral ethanol solution.

majority of the product was $A_2CHC_6H_4R$ and not $ACH(OH)C_6H_4R$, showing that the reaction: $A_2CHC_6H_4R + RC_6H_4CHO \Leftrightarrow 2ACH(OH)C_6H_4R$, observed when formaldehyde was the reactant, was not important with the aromatic aldehydes. Thus, the reaction sequence studied in this work consisted of the two reactions given below, governed by the rate constants k_1 and k_2.

All experimental evidence supported this reaction scheme providing the reaction was carried out in dilute HCl solution. Experimentally it was found that k_2 was much larger than k_1, and both reactions were kinetically second order. Under the conditions employed, only a small fraction of AH is protonated. The substituents on benzaldehyde were all *para* with R = H, CH_3, OH, OCH_3, Cl. The wavelengths used for the kinetic investigations were at or near the peak for each product: R = H, 375.5; OH, 425.0; OCH_3, 418.5; CH_3, 382.3; Cl, 377.7 nm.

The method of calculating the rate constants

As in the analogous Nioyl studies,[4] we were not able to separate the intermediate hydroxy product in a pure state and thus investigate the two reaction steps independently. The initial qualitative experiments made it clear that step 2 (k_2) was much faster than the first step (k_1) under all experimental conditions. Thus, when the aldehyde was in small excess the rate constant for the first step could be evaluated by the first-order integrated expression. This gave excellent linear relationships with reproducible first-order rate constants which were converted to second-order rate constants utilizing the aldehyde concentration. Since the intermediate complex could not be obtained in pure state, it was necessary to use a computational iterative fitting procedure to obtain both k_1 and k_2 from data at higher aldehyde concentrations.

The reaction is of a typical competitive consecutive second-order process. For this type of sequence there are many discussions available on the methods of calculation of the rate constants from experimental data,[7-11] but all of them are complicated and relatively inaccurate. We chose to apply an iterative fitting method by which the two rate constants could be obtained. The results of these evaluations agreed with the independently determined rate constant for the first step.

The reactions may be expressed as follows:

$$AH + ald \xrightarrow{k_1} B, \quad AH + B \xrightarrow{k_2} C,$$

where ald = aldehydes, B = $ACH(OH)C_6H_4R$ and C = $A_2CHC_6H_4R$. The rate equations may be written as $d[AH]/dt = -k_1[ald]_0[AH] - k_2[AH][B]$;

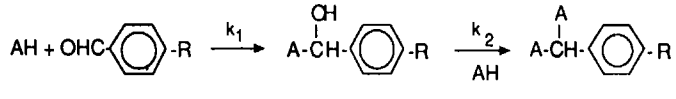

$d[C]/dt = k_2[AH][B]$ and for material balance $[B] = [AH]_0 - [AH] - 2[C]$. Then one obtains $d[AH]/dt = k_1[ald][AH] - k_2[AH]([AH]_0 - [AH] - [C])$; and $d[C]/dt = k_2[AH]([AH]_0 - [AH] - 2[C])$. Letting $[AH]_r = [AH]/[AH]_0$, $[C]_r = 2[C]/[AH]_0$ and $[ald]_0 \gg [AH]_0$, we obtain

$$d[AH]_r/dt = -k'_1[AH]_r - k'_2[AH]_r(1 - [AH]_r - [C]_r) \quad (1)$$

and

$$d[C]_r/dt = k'_2[AH]_r(1 - [AH]_r - [C]_r). \quad (2)$$

From the absorbance at a suitable wavelength, $[C]_r$ may be determined:

$$[C]_r = \Delta A/\Delta A_\infty = (A_t - A_0)/(A_\infty - A_0). \quad (3)$$

By means of eqs (1)–(3) the rate constants were determined from absorbance versus time data by the following computer program sequence:

(1) Approximate assumed values of k'_1 and k'_2 are substituted into eqs (1) and (2) which are solved by the Runge–Kutta method[12] to obtain a series of $[C]'_r$ values at different times.

(2) The $[C]'_r$ values were compared with the experimental $\Delta A/\Delta A_\infty$ values and the standard least square deviation, S, calculated.

(3) Using the Gauss–Newton–Marquardt non-linear iterative fitting method,[13] the k'_1 and k'_2 values which gave the minimum S values were determined, which are the rate constants required.

Experimental and calculated values of [C] and standard deviations in each parameter were obtained. A representative graph for one run is given in Fig. 4. In general, the estimated error in k'_1 was about $\pm 3\%$ and for k'_2 about ± 5–10%.

The fit to the experimental data was excellent and replicate runs agreed quite well, especially for k'_1. Agreement between the values for k'_1 determined by the pseudo-first-order method and the $k'_1 + k'_2$ iterative method were very good, suggesting that reliance can be placed on both.

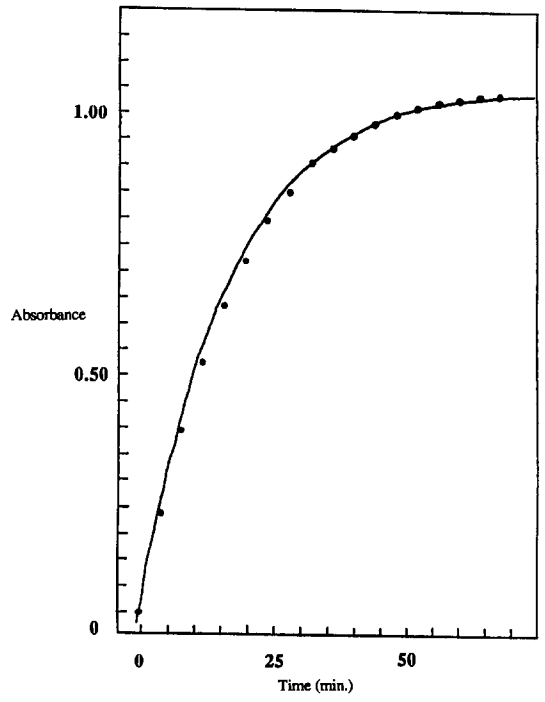

Fig. 4. Gauss–Newton–Marquardt iterative fit to a set of data. Line, calculated; dots, experimental.

RESULTS AND DISCUSSION

Aldehyde dependence

In all cases the aldehyde was present in excess of [AH] and values were determined for k'_1 by the pseudo-first-order method and also by the iterative method for k'_1 and k'_2. The values for k'_2 are generally about 25 times the corresponding values for k'_1, in agreement with our qualitative preliminary observations. The observed values for k'_1 were directly related to the initial concentration of the aldehyde (Table 1) in all cases and the linearity of the dependence was excellent. There is no zero-order term as shown by the lack of a significant intercept in the graph shown in Fig. 5. However, k'_2 did not change significantly with changes in aldehyde concentration, as expected, and in fact was not very sensitive to substitutions on the aldehyde itself. The k'_1 values were a function of the substituent on the aldehyde, with the larger rate constants occurring with the electron-donating groups in the *para* position.

Acid dependence

Because side reactions (product oxidation) and dissociation (hydrolysis of the C=N bonds) compete with the reactions being studied in low acid media, it was necessary to study the system in a higher but narrow range of acidities (0.02–0.12 M) where there was no significant interference. Both side reactions produce products which have very large extinction coefficients in the lower energy visible region and thus can be observed even if present only in trace amounts.

Tables 1 and 2 give the values for k'_1 and k'_2 for the series of aldehydes at different acidities. For each of the substituted aldehydes there was a linear relationship between the rate constant of the first step and the hydrogen ion concentration, which leads to the values in Table 3 for k_{1h}. The extrapo-

Table 1. Rate constants k'_1 and k'_2 as a function of [aldehyde] (36.1°C, [HCl] = 0.0544 M, [AH] = 4.51×10^{-3} M)

R	$10^3 \times [ald_0]$	k'_1 (min^{-1})	k'_2 (min^{-1})	$10^2 \times S$
OH	3.03	0.0600	2.48	0.290
	4.03	0.0742	2.49	0.348
	5.02	0.0880	2.48	0.545
	6.00	0.102	2.48	0.665
OCH_3	5.10	0.0640	2.05	0.502
	6.30	0.0775	2.01	1.35
	6.99	0.0850	2.09	1.19
	7.68	0.0939	2.10	1.04
CH_3	7.60	0.0962	2.44	0.929
	10.1	0.119	2.45	0.625
	12.0	0.135	2.45	0.577
	15.3	0.165	2.43	0.657
H	7.62	0.0650	1.00	0.845
	11.2	0.0988	1.02	0.945
	14.5	0.120	0.999	1.35
	17.8	0.149	1.02	1.76
Cl	6.96	0.0650	0.955	1.05
	10.4	0.0840	0.954	1.00
	13.8	0.102	0.964	1.16
	17.3	0.120	0.920	1.95

* r was always greater than 0.999.

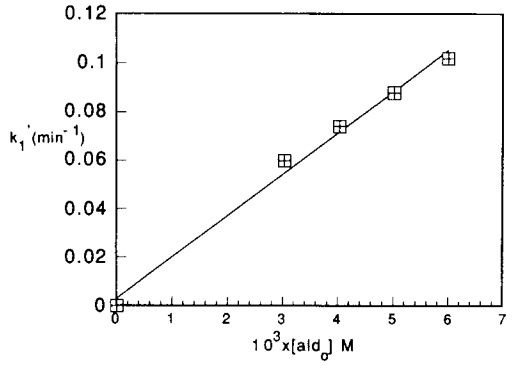

Fig. 5. k'_1 versus [aldehyde]. R = OH, 36.1°C, 0.0544 M HCl, [AH] = 4.51×10^{-3} M.

lated intercepts at zero acidity, k_{1o}, are significant and parallel the values for k_{1h}. Thus, the k_1 term is zero and first order in $[H^+]$ and both terms have a large effect on the observed rates. At least where measured (R = OH), k_2 also is composed of the same two rate terms. The cause of the acid dependence cannot be determined unambiguously. Both the aldehydes and AH are capable of being protonated. The basicities of the aldehydes and AH are small, however, and a major fraction of AH is not protonated at the acidities employed. The aldehydes are even weaker bases and require higher acidities to have a major fraction protonated. The site of protonation on AH is far from the reacting carbon [C(12)] and X-ray structural data on $AH_2^+ClO_4^-$ shows[14] little change in the bond distances and angles around C(12) upon protonation at the oxime hydrogen bond. Thus, we suggest that protonation of AH at the hydrogen bond has little effect on the rate of reaction of aldehydes and that the acid dependence is due predominantly to protonation at the carbonyl oxygen of the aldehyde. The hydrogen ion dependence of k_1 is summarized in Table 3, where the slopes (k_{1h}) and intercepts (k_{1o}) of graphs of k_1 versus $[H^+]$ are given. Because of the limited precision of values of k_2, the hydrogen ion dependency was not measured and k_{2o} and k_{2h} were not evaluated.

The effect of aldehyde para-*substituents*

Table 3 lists the observed rate constants, k_1, k_{1h} and k_{1o} for the different aldehydes used in this study. Figure 6 shows a graph of the values of $\ln(k_{1h})$ versus the Hammett S parameters of the substituents. There is a clear correlation, $R = 0.998$, which is in agreement with the concept of viewing the acid-dependent path for this reaction being favoured by low electron density on the protonated aldehyde. This is the same behaviour observed when Nioyl was the nucleophile.[4] The acid-independent term is viewed in the same manner, utilizing the unprotonated aldehyde as the electrophile. A comparison

Table 2. Acidity dependence of k_1 and k_2 (28.2°C, M^{-1} s^{-1})

R	[HCl], M =	0.024	0.048	0.072	0.096	0.110
OH	k_1	0.206	0.279	0.331	0.402	0.464
OCH_3	k_1	0.207	0.258	0.330	0.370	0.436
CH_3	k_1	0.191	0.240	0.283	0.339	0.389
H	k_1	0.160	0.200	0.237	0.273	0.314
Cl	k_1	0.0797	0.109	0.136	0.160	0.194
OH	k_2	361	482	540	561	626

Table 3. Linear hydrogen ion dependence of k_1 giving k_{1h} (28.2°C)

R =	OH	OCH_3	CH_3	H	Cl
k_{1h} (M^{-2} s^{-1})	2.88	2.70	2.03	1.72	1.17
k_{1o} (M^{-1} s^{-1})	0.135	0.136	0.141	0.116	0.054
k_2 (M^{-1} s^{-1})	626	686	624	776	87 (0.11 M HCl)

Table 4. Effect of water–ethanol composition

% H_2O (v/v)	55	64	72	80	88
[Benzaldehyde]					
k_1 (M^{-1} s^{-1})	0.0826	0.129	0.172	0.220	0.289
k_2 (M^{-1} s^{-1})	34.6	56.1	85.7	172	364
CH_3-phenylCHO					
k_1 (M^{-1} s^{-1})	0.140	0.192	0.251	0.356	0.577
k_2 (M^{-1} s^{-1})	181	223	419	671	873

Table 5. Values of k_1 versus temperature (in units of M^{-1} s^{-1})

T (°C) R =	OH	OCH_3	CH_3	H	Cl
36.1	0.237	0.192	0.148	0.127	0.089
41.4	0.271	0.229	0.187	0.149	0.125
46.5	0.329	0.259	0.226	0.170	0.150
51.4	0.382	0.296	0.254	0.198	0.193

Table 6. Kinetic activation parameters

R =	OH	OCH_3	CH_3	H	Cl
$\Delta H^{\ddagger}$ (kJ mol^{-1})	23.9±0.8	20.7±0.8	27.0±1.4	21.4±1.2	38.4±3
$\Delta S^{\ddagger}$ (J K^{-1} mol^{-1})	−179±2	−192±4	−173±4	−193±9	−141±0.3
r	0.996	0.998	0.992	0.999	0.994

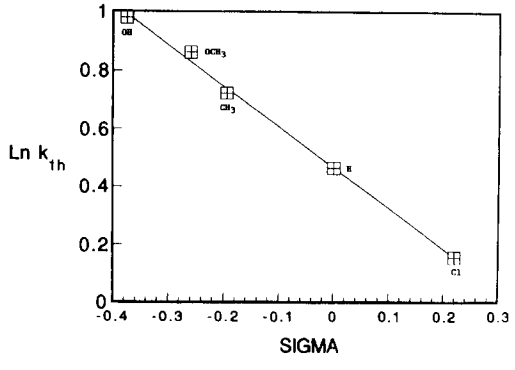

Fig. 6. Correlation of $\ln(k_{1h})$ versus the Hammett S parameter.

of Ptoyl with Nioyl shows the nickel(II) analogue to be the more reactive and thus we would presume it has a larger negative charge on the C(12) atom.

The effect of changing solvent

The ratio of water to alcohol in the solvent strongly affected the observed rate constants. When all other conditions remain constant, increasing the water content increases both k_1 and k_2. The results are listed in Table 4. While this may be a manifestation of a change in A_{H^+}, it was not apparent with the glass electrode because the measured pH

changed only slightly for the different ethanol–water solutions.

Temperature effect

The effect of temperature was measured for the first step, k_1, only because insufficient accuracy was possible with step 2 to allow the calculation of reliable activation parameters. The measured values of k_1 are given in Table 5 and the derived activation parameters in Table 6.

The rate equation for the first step is rate $= k_1[AH][ald][H^+]$. The rate constant increases with increasing electron donor ability of groups in the *para* position of the benzene ring of the aldehyde and increases with a higher water content of the solvent. If one assumes that effective protonation occurs on the aldehyde oxygen (not on the OHO of AH), then the following activated state geometry is attractive. This suggests that the most important

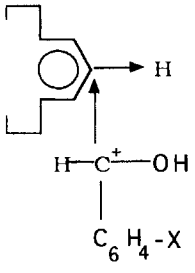

process leading to the activated state is the protonation of the aldehyde oxygen, which is facilitated by electron-donating groups on the benzene ring. k_{1h} would then be equal to $K_H k_p$, where K_H is the protonation constant of the aldehyde and k_p is the rate constant for the protonated aldehyde reacting with AH. The increased positive charge on the aldehyde carbon increases its tendency to interact with electron-rich C(12) to give $ACH(OH)(C_6H_4R)$. Thus, we interpret the kinetic results in terms of the electron-donating ability of substituents on the benzene ring changing the protonation constant of the aldehyde and increasing the fraction of aldehyde in the protonated state. The solvent effect cannot be interpreted definitively at this time.

The second step shows no aldehyde dependence and terms zero and probably first order in acidity. In this case the protonation of $ACH(OH)(C_6H_4R)$ could lead to $A{=}CH(C_6H_4R)$, which would be the reactant toward AH. Nothing is known about the rate of water loss or the protonation constants needed to predict this behaviour.

The activation parameters for k_1 given show fairly consistent behaviour with a fairly high value (around 25 kJ mol^{-1}) for the activation enthalpy change and a very large value (around 170 kJ^{-1} mol^{-1}) for the activational entropy change. These are similar to those observed in the Nioyl studies for the analogous reaction, where again the chloro derivative is somewhat unique.

REFERENCES

1. I. O. Uban and E. G. Vassian, *Inorg. Chem.* 1979, **18**, 867.
2. A. F. Ghiron, R. K. Murmann and E. O. Schlemper, *Inorg. Chem.* 1985, **24**, 3271.
3. Qi-Yan Zhang, Bin Song, Yun-Ti Chen and R. Kent Murmann, *Inorg. Chem.* 1992, **31**, 2314.
4. Yuan-Ming Zhang, Yun-Ti Chen and R. Kent Murmann, *J. Indian Chem. Soc.* 1992, **69**, 420.
5. E. G. Vassian and R. K. Murmann, *Inorg. Chem.* 1967, **6**, 2043.
6. R. K. Murmann, E. O. Schlemper and M. S. Tempesta, *Polyhedron* 1986, **5**, 1647.
7. C. K. Ingold, *J. Chem. Soc.* 1931, 2170.
8. W. C. Schwemer and A. A. Frost, *J. Am. Chem. Soc.* 1951, **73**, 4541; 1952, **74**, 1286.
9. J. Drbus and C. F. Eckert, *J. Am. Chem. Soc.* 1958, **80**, 5948.
10. V. O. Rekhsfield and V. A. Prokhorova, *Kinet. Katal.* 1963, **4**, 483.
11. F. A. Kundell, D. J. Robinson and W. J. Svibely, *J. Phys. Chem.* 1973, **77**, 1552.
12. Zhuhong Zhang and Jun Zhu, *Basic Programs*, Vol. 132. Qinghua Univ. Publ. House, Qinghua University, Beijing (1980).
13. Xuansan Cai, *Optimization and Optimum Control*, Vol. 281. Qinghua Univ. Publ. House, Qinghua University, Beijing (1983).
14. E. G. Vassian and R. K. Murmann, *Coord. Chem. Rev.* 1990, **105**, 1.